

## Comparison of the effects of linking diglycidyl ether-terminated PDMS and BPA onto polyurethane with respect to the tensile and thermal properties

Yong-Chan Chung,<sup>1</sup> Kyung Hoon Chung,<sup>2</sup> Byung Hee Lee,<sup>2</sup> Byoung Chul Chun<sup>2</sup>

<sup>1</sup>Department of Chemistry, The University of Suwon, Hwaseong, Korea

<sup>2</sup>School of Nano Engineering, Inje University, Gimhae, Korea

Correspondence to: B. Chul Chun (E-mail: bcchun@inje.ac.kr)

**ABSTRACT:** Flexible poly(dimethylsiloxane) (PDMS) or rigid bisphenol A (BPA) with diglycidyl ether end groups was linked to polyurethane (PU), which was composed of 4,4'-methylenebis(phenyl isocyanate) as a hard segment and poly(tetramethylene ether)glycol as a soft segment. A control PDMS (CPDMS) series was prepared with an additional deprotonation step by NaH. The spectroscopic, thermal, tensile, shape memory, and low-temperature flexibility properties were compared with those of plain PU to investigate the effects of linking the flexible PDMS or the rigid BPA on PU. The soft segment melting peaks were not affected by the PDMS content for the PDMS series but disappeared as the BPA content increased in the BPA series. The soft segment crystallization of PU was completely disrupted as the linked BPA content increased in the differential scanning calorimetry results and disappeared in the dynamic mechanical analysis results. The glass transition temperature ( $T_g$ ) of the BPA series increased with increasing BPA content, whereas that of the PDMS series remained the same. The tensile strength of the PDMS series sharply increased with increasing PDMS content. The shape retention of the BPA series at  $-25\text{ }^\circ\text{C}$  sharply decreased as the BPA content increased. Finally, the BPA series linked with rigid aromatic BPA demonstrated excellent low-temperature flexibilities compared with the PDMS series and plain PU. Compared with PUs linked with PDMS, PUs linked with rigid BPA demonstrated a significant change in the cross-link density, thermal properties, shape retention, and low-temperature flexibility. © 2016 Wiley Periodicals, Inc. *J. Appl. Polym. Sci.* **2016**, *133*, 43284.

**KEYWORDS:** grafting; mechanical properties; polyurethanes; stimuli-sensitive polymers; structure–property relations

Received 5 August 2015; accepted 29 November 2015

DOI: 10.1002/app.43284

### INTRODUCTION

Bisphenol A (BPA) is used in industrial applications primarily for the manufacture of polycarbonate, which is a transparent and impact-resistant thermoplastic material that is used in automotive components, safety glasses, data storage disks, and beverage containers. Another major use of BPA is as an epoxy resin adhesive when the phenol hydroxyl group is converted to the diglycidyl ether end group using epichlorohydrin. The minor uses of BPA are for the production of fire retardants and thermal paper and as a plasticizer for poly(vinyl chloride).<sup>1</sup> Polymer plasticizers containing BPA are thought to disrupt the polymer chains, thus improving the cold flex temperature and the compound processing.<sup>2</sup> BPA is rarely used for polyurethane (PU) synthesis; however, bisphenol S, a similar variant of BPA that contains a sulfoxyl group instead of methylene, was reported for PU synthesis to improve its physical and thermal properties.<sup>3</sup> In contrast, polydimethylsiloxane (PDMS) has been frequently used in the synthesis of PU to exploit the excellent tensile

properties and high shape recovery of PU, as well as the resiliency and low-temperature flexibility of PDMS. For example, PDMS was used as a soft segment in PU synthesis because of its low surface tension, low glass transition temperature, and biocompatibility.<sup>4</sup> Poly(ethylene glycol) (PEG) was covalently attached to PDMS-PU using the hydrophilicity of PEG to deter the platelet and protein adhesion for biomedical applications.<sup>5</sup> PDMS-PU was used to develop a vascular graft because of the flexibility and tensile strength of PU and because of the oxidative stability and blood compatibility of PDMS.<sup>6</sup> A hyperbranched polyester with hydroxyl end groups was used as a cross-linking agent to improve the mechanical properties of PDMS-PU for coating applications.<sup>7</sup>

Recently, the modification of PU has improved its biocompatibility,<sup>8,9</sup> hydrophilicity,<sup>10</sup> pH sensitivity,<sup>11</sup> and antimicrobial activity.<sup>12</sup> Due to its excellent shape recovery, impact and scratch resistance, and flexibility, PU has a broad range of industrial applications, including coatings, glue, gaskets,

**Table I.** Composition of the PDMS- or BPA-Linked PU Series Including Plain PU

Sample code	Reactant (mmol)							
	MDI-1	PTMG	MDI-2	BD	Gly <sup>a</sup>	NaH	PDMS <sup>b</sup>	BPA <sup>c</sup>
L	20	20	30	30	-	-	-	-
PDMS-1	20	20	30	30	-	-	1.25	-
PDMS-2	20	20	30	30	-	-	2.5	-
PDMS-3	20	20	30	30	-	-	3.75	-
PDMS-4	20	20	30	30	-	-	5.0	-
PDMS-5	20	20	30	30	-	-	6.25	-
BPA-1	20	20	30	27.5	2.5	-	-	2.5
BPA-2	20	20	30	25	5.0	-	-	5.0
BPA-3	20	20	30	22.5	7.5	-	-	7.5
BPA-4	20	20	30	20	10	-	-	10
BPA-5	20	20	30	15	15	-	-	15
CPDMS-1 <sup>d</sup>	20	20	30	30	-	1.25	1.25	-
CPDMS-3	20	20	30	30	-	3.75	3.75	-
CPDMS-5	20	20	30	30	-	6.25	6.25	-

<sup>a</sup>Glycerol<sup>b</sup>Poly(dimethylsiloxane) with diglycidyl ether end groups (PDMS) and<sup>c</sup>Bisphenol A with a diglycidyl ether end group (BPA) were used.<sup>d</sup>The CPDMS series used NaH as a base to catalyze the linking process.

stretchable textile fibers, mattress foams, construction sealants, medical tubes and catheters, and automobile interior components.<sup>13–15</sup> The interactions between PU chains, such as hydrogen bonding and dipole–dipole interactions, maintain its high shape recovery rate and tensile strength. However, the molecular interactions could be disrupted by the attachment of rigid and bulky side groups to PU, and the low-temperature flexibility of PU could be improved by using its weak molecular interactions.<sup>16</sup> Polymers with low-temperature flexibility have been used in many industrial applications, such as insulation/protection materials for pipes and tanks that carry liquid natural gas, petrochemicals, and industrial gases; low-temperature sealing devices for drilling applications at high latitudes; electric cable insulation and jacketing that are flexible at very low temperatures; and water suction and discharge hoses that remain flexible at extremely low temperatures.<sup>17,18</sup> PUs that function with a different low-temperature flexibility mechanism from those of previously studied polymers and that demonstrate high tensile strength and shape memory properties were prepared and investigated in this study. Specifically, the flexible PDMS or the rigid BPA was linked as a side group to PU using the reactive epoxy end groups, and the effects and differences of the linked BPA or PDMS on the tensile strength, shape memory, and low-temperature flexibility of PU were analyzed.

## EXPERIMENTAL

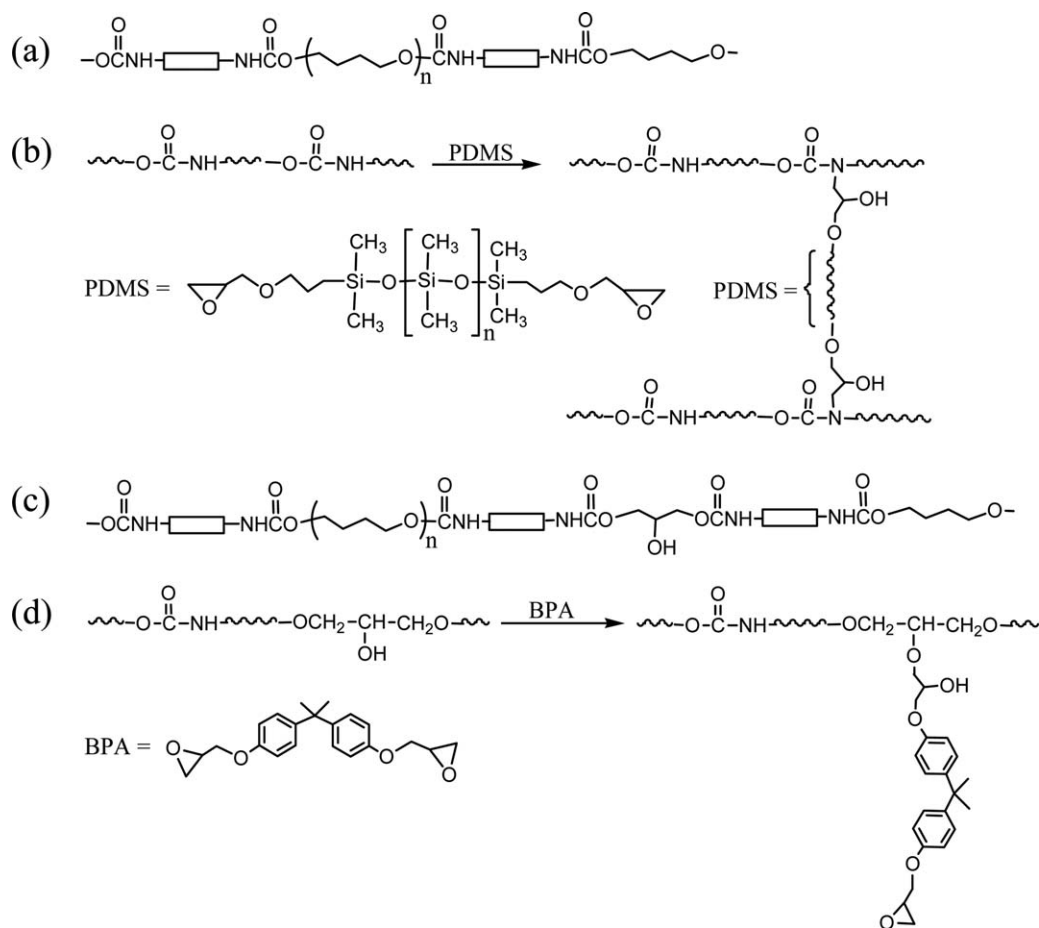
### Materials

Poly(tetramethylene ether)glycol (PTMG,  $M_n \sim 2000$  g/mol, Sigma-Aldrich, St Louis, MO), 4,4'-methylenebis(phenyl isocyanate) (MDI, Junsei Chemical, Tokyo, Japan), glycerol (Junsei Chemical), and 1,4-butanediol (BD, Junsei Chemical) were dried

overnight in a high vacuum atmosphere (0.1 torr). Diglycidyl ether-terminated poly(dimethylsiloxane) (PDMS,  $M_n \sim 800$  g/mol, Sigma-Aldrich), diglycidyl ether-terminated bisphenol A (BPA, Sigma-Aldrich), and sodium hydride (Sigma-Aldrich) were used as received. Dimethylformamide (DMF, Duksan Chemical, Ansan, Korea) was distilled over  $\text{CaH}_2$  before use.

### PU Synthesis

The following PU synthesis was based on previous methods.<sup>19,20</sup> MDI (MDI-1, 5.00 g, 20.0 mmol) was added to PTMG (40.0 g, 20.0 mmol) in a 500-mL four-necked beaker-type flask equipped with a mechanical stirrer, condenser, temperature-controlled heating mantle, and nitrogen purge. The mixture was allowed to react for 2 h at 50 °C to prepare the prepolymer. BD, in the amount shown in Table I, was dissolved in 10 mL of DMF and was added to the prepolymer. The mixture was allowed to react for 1 h. MDI (MDI-2, 7.50 g, 30.0 mmol) was added to the reaction mixture, and the reaction was continued for 1 h; 10 mL of DMF was slowly added during the reaction via a dropping funnel to prevent a sudden increase in viscosity. After PDMS in 10 mL of DMF was added to the reaction mixture, the reaction continued for 3 h. The synthesis of the control series, the CPDMS series, proceeded in the same manner as that of the PDMS series, except that a dispersion of NaH in 10 mL of DMF was added to the reaction mixture after the addition of PDMS. The amounts of PDMS and NaH are shown in Table I. Regarding the BPA series, the PU synthetic steps followed the method for the PDMS series, except that an amount of glycerol, as shown in Table I, was added with the BD, and BPA was used instead of PDMS. After the reaction period, the product was precipitated in distilled water (1.5 L) to terminate polymerization. The product was cut into pieces and thoroughly



**Scheme 1.** (a) Structure of PU (the rectangle represents MDI), (b) cross-linking of PU with diglycidyl ether-terminated PDMS, (c) structure of PU incorporating glycerol, and (d) linking of PU with diglycidyl ether-terminated BPA.

washed with magnetic stirring in distilled water ( $1.5 \text{ L} \times 3$ ) and ethanol ( $1 \text{ L} \times 2$ ) to remove any remaining reactants. The final product was suction filtered and dried in an oven ( $60^\circ\text{C}$ ) for 3 days. The PU structure and the linking of PDMS or BPA to PU are shown in Scheme 1. Specimens for mechanical and shape memory testing were prepared by solvent casting. Specifically, a solution of PU in DMF was slowly evaporated at  $60^\circ\text{C}$  for 60 h to obtain a sheet (0.5 mm thick). The film thickness was measured using a digital caliper (Mitutoyo CD-15CPX, Tokyo, Japan), and the average thickness from five points was recorded. Specimens were prepared from the PU sheet according to ASTM D638.

#### Cross-Link Density

A specimen with the dimensions of  $20 \times 20 \times 1 \text{ mm}$  and a known weight ( $m_1$ ) was allowed to swell in 50 mL of toluene in a closed cap bottle for 24 h. The swollen weight of the specimen ( $m_2$ ) was measured after quickly removing the adsorbed toluene from the polymer surface with a tissue. The swollen specimen was dried at room temperature for 1 week and then weighed to obtain a dry mass ( $m_3$ ). The solvent volume ( $V_s$ ) of the swollen specimen, averaged over five swelling experiments, was calculated using the weight difference between the swollen ( $m_2$ ) and dry states ( $m_3$ ) and the solvent density ( $0.8699 \text{ g/cm}^3$ ). The volume

of the polymer ( $V_p$ ) in its dry state was calculated by dividing the polymer dry weight ( $m_1$ ) by the polymer density. The volume fraction of polymer in the swollen mass ( $v_1$ ) was calculated using the equation  $V_p/(V_s + V_p)$ . The derivation of the cross-link density is described in the Results and Discussion section.

#### Tensile and Shape Memory Test

The tensile mechanical properties were measured according to the ASTM D638 standard at  $25^\circ\text{C}$  using 0.5-mm-thick samples. Testing was performed on a universal testing machine (UTM, LR10K, Lloyd Materials Testing, West Sussex, UK) with the following parameters: 20-mm gauge length, 20 mm/min crosshead speed, and 0.5 kN load cell. Seven specimens were tested for each group; the tensile properties were determined as the average of 5 specimens, excluding the highest and lowest values. The same UTM equipped with a temperature-controlled chamber was employed for shape memory test. A sample with length  $L_0$  was drawn 100% to  $2L_0$  in a temperature-controlled chamber set to  $45^\circ\text{C}$ . This test was performed over the course of 2 min, and the sample was maintained at  $45^\circ\text{C}$  for 5 min. The upper grip was released after the specimen in the chamber was cooled with liquid nitrogen to  $-25^\circ\text{C}$  for 10 min. The shrunken length ( $L_1$ ) of the sample was measured once the temperature remained at  $-25^\circ\text{C}$  for 10 min. The percent shape retention

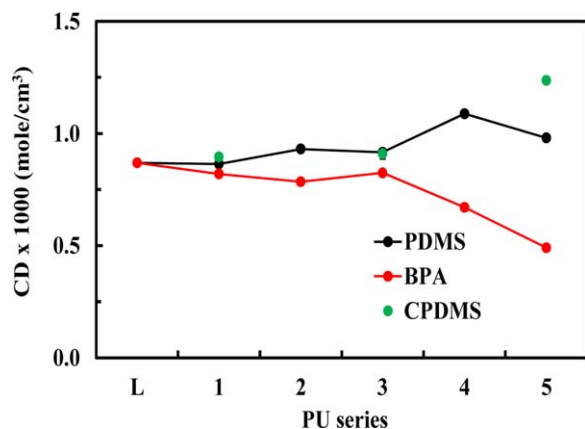


**Figure 1.** Cross-link density profiles of the PDMS, BPA, and CPDMS series. [Color figure can be viewed in the online issue, which is available at [wileyonlinelibrary.com](http://wileyonlinelibrary.com).]

(%) was then calculated using eq. (1),  $L_0$ , and  $L_1$ . In the chamber, the specimen was heated to 45 °C for 10 min; subsequently, the length ( $L_2$ ) was measured. The percent shape recovery (%) was then calculated using eq. (2),  $2L_0$ , and  $L_2$ .

$$\text{Shape retention} = (L_1 - L_0) \times 100 / L_0 (\%) \quad (1)$$

$$\text{Shape recovery} = (2L_0 - L_2) \times 100 / L_0 (\%) \quad (2)$$

### Characterization

A Fourier-transform infrared spectrophotometer (JASCO 300E, Tokyo, Japan) equipped for attenuated total reflectance measurements was used to collect the infrared spectra. For each sample, 25 scans were taken at a 4  $\text{cm}^{-1}$  resolution and a scan speed of 2 mm/s. A differential scanning calorimeter (DSC, TA instruments DSC-Q20, New Castle, DE) was used to obtain calorimetry data for heating and cooling scans at a rate of 10 °C/min between -50 and 250 °C. The PU sample (5 mg) was heated to 250 °C and cooled to -50 °C after being held at 250 °C for 5 min. The sample was heated again to 250 °C at 10 °C/min and monitored for phase transitions. The soft segment melting temperature ( $T_m$ ) during the heating scan and the enthalpy change of melting ( $\Delta H_m$ ) were determined using Platinum™ software, which was included with the DSC instrument. Dynamic mechanical analysis was used to collect the glass transition data at low temperatures. These measurements were obtained using a dynamic mechanical analyzer (DMA, Triton TTDMA, Lincolnshire, UK) to measure the storage modulus and loss modulus in a tension mode between -150 and 100 °C at 10 Hz. The low-temperature flexibility test was conducted in a temperature-controlled chamber of the UTM for a twisted spiral sample frozen at -35 °C for the PDMS series and at -45 °C for the BPA series for 3 h and was recorded using a video camera (SONY HDR-CX 550, Tokyo, Japan) installed close to the chamber window while the temperature was increased by 10 °C/min.

## RESULTS AND DISCUSSION

### PU Structure

The two PU series, the PDMS and BPA series, share MDI and PTMG as the hard and soft segments, respectively, and BD as a chain extender. The PDMS series was linked with PDMS

containing the epoxy end groups in which the carbamate bonding of PU was used as the site for linking.<sup>21</sup> The linked PDMS could be used for the light cross-linking of PU chains due to the bifunctional glycidyl end groups of PDMS, as shown in Scheme 1(b). In the control CPDMS series, NaH was used to deprotonate the carbamate bonding to aid the linking step. However, the BPA series differed from the PDMS series regarding the replacement of some of the BD with glycerol. Glycerol was incorporated into PU to provide a free hydroxyl group that was used as a linking site for BPA. The glycerol and BPA content of the BPA series slowly increased (shown in Table I), and the total molar content of glycerol and BD in this series was the same as that of MDI-2. The free hydroxyl group from glycerol reacted with the epoxy end group of BPA to form a link to PU, as shown in Scheme 1(d); in addition, light cross-linking was also possible for the BPA series due to the bifunctional glycidyl end groups. PDMS was selected to link a flexible chain to PU because PDMS is known to be very resilient at low temperatures and has a remarkably low glass transition temperature (-123 °C). In contrast, BPA has a rigid aromatic structure similar to that of the MDI hard segment and may disrupt the PU chain alignment and packing. The linking of either PDMS or BPA with diglycidyl end groups to PU is expected to increase the tensile strength via the light cross-linking and change the thermal properties from those of plain PU (L). The appearances of the casted films of the PDMS and BPA series revealed a homogeneous PU surface, which suggests that the aggregation of PU chains due to the linked PDMS or BPA did not occur. It will be of interest to compare the effects of PDMS and BPA linking on the thermal, mechanical, and low-temperature flexibility properties of PU (Figure 1).

To test the possibility of light cross-linking due to the linking of PDMS and BPA, the degree of cross-linking was determined using the PU swelling method in toluene in which the PU swelling was inversely related to the degree of cross-linking. Specifically, the interaction parameter ( $\chi$ ) between toluene and PU was determined from the following expression<sup>22</sup>:

$$\chi = (\delta_1 - \delta_2)^2 V_1 / RT$$

$$\chi = \text{interaction parameter}$$

$$\delta_1 \text{ and } \delta_2 = \text{solubility parameter of solvent and polymer} \quad (3)$$

$$V_1 = \text{molar volume of solvent (106.3 cm}^3/\text{mol)}$$

$$R = \text{gas constant (8.31 MPa} \cdot \text{cm}^3 \cdot \text{K}^{-1} \cdot \text{mol}^{-1})$$

$$T = \text{absolute temperature (298 K)}$$

The solubility parameters of toluene ( $\delta_1$ ) and PU ( $\delta_2$ ) are 18.2 and 20.5 (MPa)<sup>1/2</sup>, respectively.<sup>23,24</sup> The cross-link density was calculated from the Flory-Rehner eq. (4):

$$-\ln(1 - v_2) + v_2 + \chi v_2^2 = V_1 n [v_2^{1/3} - 1/2 v_2]$$

$$v_2 = \text{volume fraction of polymer in the swollen mass} \quad (4)$$

$$n = \text{cross-link density}$$

The cross-link density of the PDMS series slightly increased as the PDMS content increased. However, the cross-link density of the BPA series was significantly decreased as the BPA content

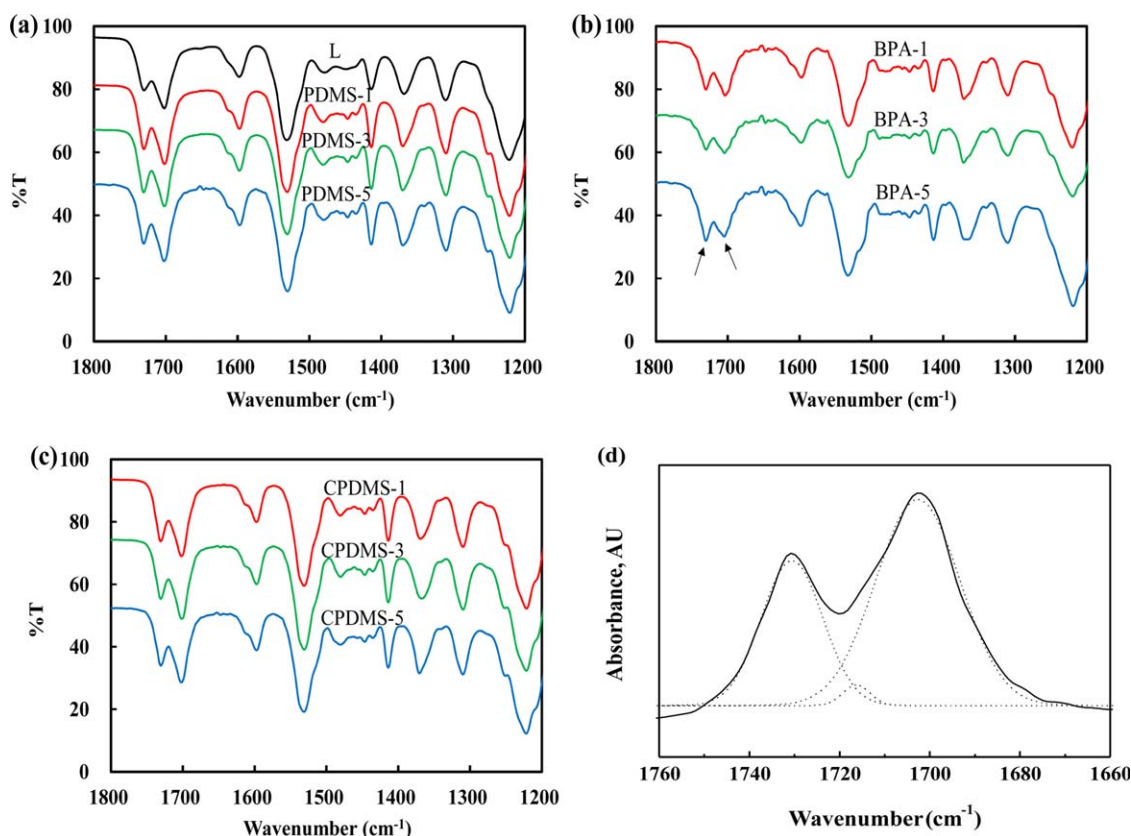


**Figure 2.** IR spectra of the (a) PDMS, (b) BPA, (c) CPDMS series, and (d) the resolution of the carbonyl absorption peaks of PDMS-5. [Color figure can be viewed in the online issue, which is available at [wileyonlinelibrary.com](http://wileyonlinelibrary.com).]

increased (Figure 1). The light cross-linking by PDMS in the PDMS series was responsible for the slight increase, whereas the disruption of the PU chain alignment by the linked BPA increased the swelling of PU and reduced the cross-link density. The contrasting cross-link density results affect the shape memory and thermal properties, as discussed in the following section.

#### IR and Thermal Analysis

The IR spectra showed peaks for C-H bending at  $1529\text{ cm}^{-1}$ , aromatic C-C ring stretching at  $1596$  and  $1413\text{ cm}^{-1}$ , O-H bending at  $1369\text{ cm}^{-1}$ , C-N stretching at  $1309\text{ cm}^{-1}$ , and C-O stretching at  $1219\text{ cm}^{-1}$  for the PDMS and CPDMS series, as well as for the BPA series (Figure 2). The C=O stretching peaks at approximately  $1700$ ,  $1712$ , and  $1730\text{ cm}^{-1}$  are used to analyze molecular interactions, such as hydrogen bonding and dipole-dipole interactions, between hard segments. The strongly bonded carbonyl stretching peak ( $1700\text{ cm}^{-1}$ ) and the weakly bonded carbonyl stretching peak ( $1714\text{ cm}^{-1}$ ) appeared at a lower wavenumber than the free carbonyl stretching peak ( $1730\text{ cm}^{-1}$ ).<sup>25,26</sup> The relative intensity between the bonded carbonyl and the free carbonyl signifies the degree of phase separation (DPS). The DPS implies a change in the molecular interaction between hard segments and is calculated using the equation [DPS = area (strongly bonded) + area (weakly bonded)/(area (strongly bonded) + area (weakly bonded) + area (free))], where area (strongly bonded), area (weakly bonded), and area (free) represent the absorbance peak areas at  $1695$ –

$1708\text{ cm}^{-1}$ ,  $1710$ – $1722\text{ cm}^{-1}$  and  $1724$ – $1742\text{ cm}^{-1}$ , respectively. The overlapped carbonyl peaks were attributed to strongly bonded carbonyl, weakly bonded carbonyl, and free carbonyl peaks, and their peak areas were compared using OriginPro 8 software [Figure 2(d)]. The DPS of the PDMS series slightly decreased from 71.6% for L to 65.7% for PDMS-5, 66.7% for PDMS-3, and 67.8% for CPDMS-5. However, the DPS of the BPA-5 series significantly decreased to 63.9%. The DPS results suggested that the molecular interactions between carbonyl groups were significantly affected by the linked BPA in the BPA series but were not influenced as much by the PDMS linking in the PDMS series.

The melting temperature ( $T_m$ ) of the soft segment in the PDMS and BPA series was investigated using DSC. The melting peak of the soft segment was observed between  $18$  and  $22^\circ\text{C}$  during the second heating scan (Figure 3). The  $T_m$  and enthalpy change ( $\Delta H_m$ ) for melting are shown in Table II. The  $T_m$  remained constant compared with that of L ( $18.7^\circ\text{C}$ ) as the PDMS content increased for the PDMS and CPDMS series. For example, the  $T_m$  of PDMS-1 ( $19.7^\circ\text{C}$ ) and CPDMS-1 ( $21.6^\circ\text{C}$ ) changed to  $21.5^\circ\text{C}$  for PDMS-5 and  $21.6^\circ\text{C}$  for CPDMS-5, respectively. However, the melting peaks for the BPA series disappeared as the BPA content increased. The  $\Delta H_m$  value did not significantly change as the PDMS content increased in the PDMS and CPDMS series:  $30.7\text{ J/g}$  for PDMS-1 and  $40.0\text{ J/g}$  for CPDMS-1 changed to  $27.3\text{ J/g}$  for PDMS-5 and  $43.9\text{ J/g}$  for CPDMS-5, respectively. The  $\Delta H_m$  of the BPA series rapidly decreased from

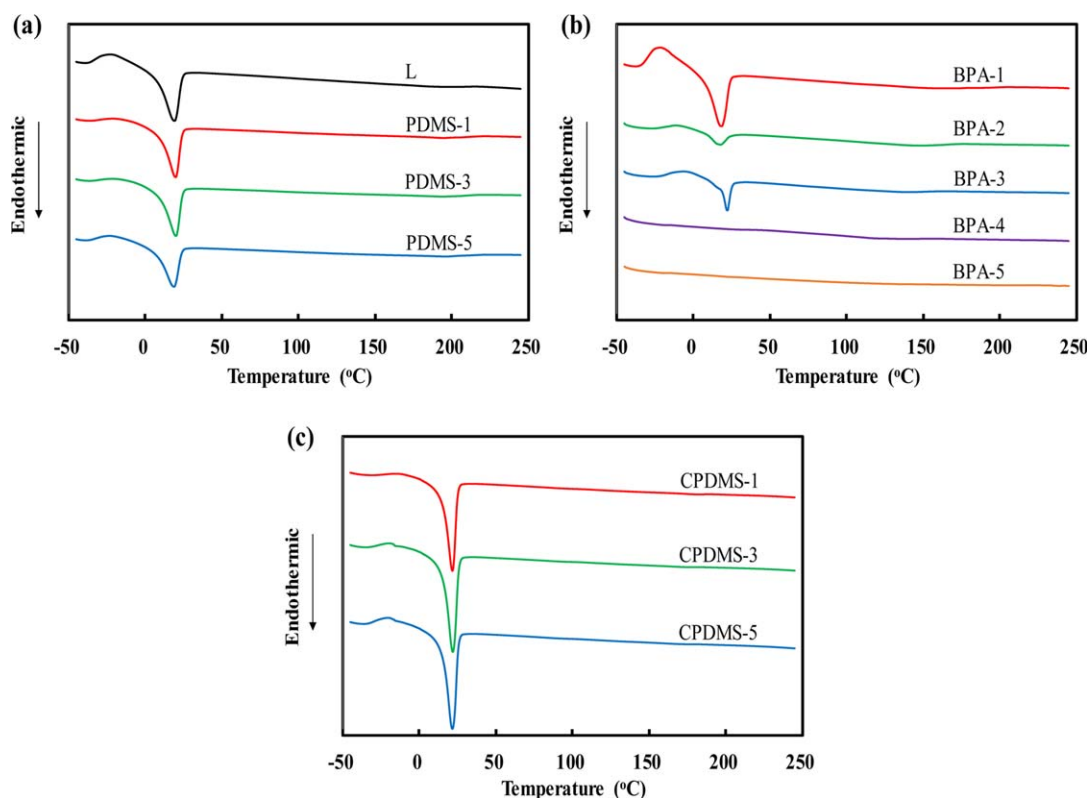


**Figure 3.** DSC heating scans of the (a) PDMS, (b) BPA, and (c) CPDMS series. [Color figure can be viewed in the online issue, which is available at [wileyonlinelibrary.com](http://wileyonlinelibrary.com).]

19.9 J/g for BPA-1 and was not detected for BPA-5. The rigid aromatic structure of the linked BPA for the BPA series disrupted the PU chain packing and resulted in the disappearance of the melting peak as the BPA content increased, whereas the resilient PDMS for the PDMS series did not exhibit an interruption of the PU chains. The cold crystallization peak of the soft segment observed at approximately  $-20^{\circ}\text{C}$  for BPA-1 completely disappeared as the BPA content increased [Figure 3(b)], revealing that the linked BPA in the BPA series disturbed the crystallization of the PTMG soft segment.<sup>27</sup> The glass transition temperature ( $T_g$ ) of the soft segment was investigated by DMA; in this investigation, the storage modulus and loss modulus were monitored between  $-150$  and  $100^{\circ}\text{C}$  (Figure 4). The rapid decrease in the storage modulus and the appearance of a loss modulus peak were observed at approximately  $-60^{\circ}\text{C}$ , which indicated the glass transition of the soft segment. The  $T_g$  data of the PDMS and BPA series in Table II were based on the loss modulus peak. The  $T_g$  data also exhibited differences between the PDMS and BPA series as the PDMS and BPA content increased. The  $T_g$  increased slightly from  $-67.0^{\circ}\text{C}$  for L to  $-64.7^{\circ}\text{C}$  for PDMS-5 in the PDMS series; however, it increased significantly to  $-57.2^{\circ}\text{C}$  for BPA-5 in the BPA series. The CPDMS series also did not exhibit a significant increase in  $T_g$  (the  $T_g$  of CPDMS-5 was  $-63.9^{\circ}\text{C}$ ). The  $T_g$  increase of the BPA series was more obvious than that of the PDMS series, which suggested that the linked BPA significantly hindered the PU chain rotation and vibration for the BPA series compared with the linked PDMS in the PDMS series. The cold crystallization

peaks for the BPA series at approximately  $-20^{\circ}\text{C}$  in Figures 4(a,b) completely disappeared as the BPA content increased, whereas those of the PDMS and CPDMS series did not exhibit decreased crystallization peaks as the PDMS content increased.

**Table II.** Comparison of the Thermal Properties of PDMS- or BPA-Linked PU Series

Sample code	$T_m$ ( $^{\circ}\text{C}$ )	$\Delta H_m$ (J/g)	$T_g$ ( $^{\circ}\text{C}$ ) <sup>a</sup>
L	18.7	28.5	$-67.0$
PDMS-1	19.7	30.7	$-63.6$
PDMS-2	19.2	28.9	$-63.8$
PDMS-3	19.9	30.3	$-63.9$
PDMS-4	17.9	25.9	$-64.2$
PDMS-5	18.7	27.3	$-64.7$
BPA-1	18.2	19.9	$-64.6$
BPA-2	17.6	4.9	$-63.3$
BPA-3	22.0	7.3	$-60.1$
BPA-4 <sup>b</sup>	-	-	$-60.2$
BPA-5 <sup>b</sup>	-	-	$-57.2$
CPDMS-1	21.6	40.0	$-64.8$
CPDMS-3	21.8	42.9	$-65.3$
CPDMS-5	21.5	43.9	$-63.9$

<sup>a</sup>  $T_g$  was determined from the loss modulus data.

<sup>b</sup> Melting peak was not detected for BPA-4 or BPA-5.

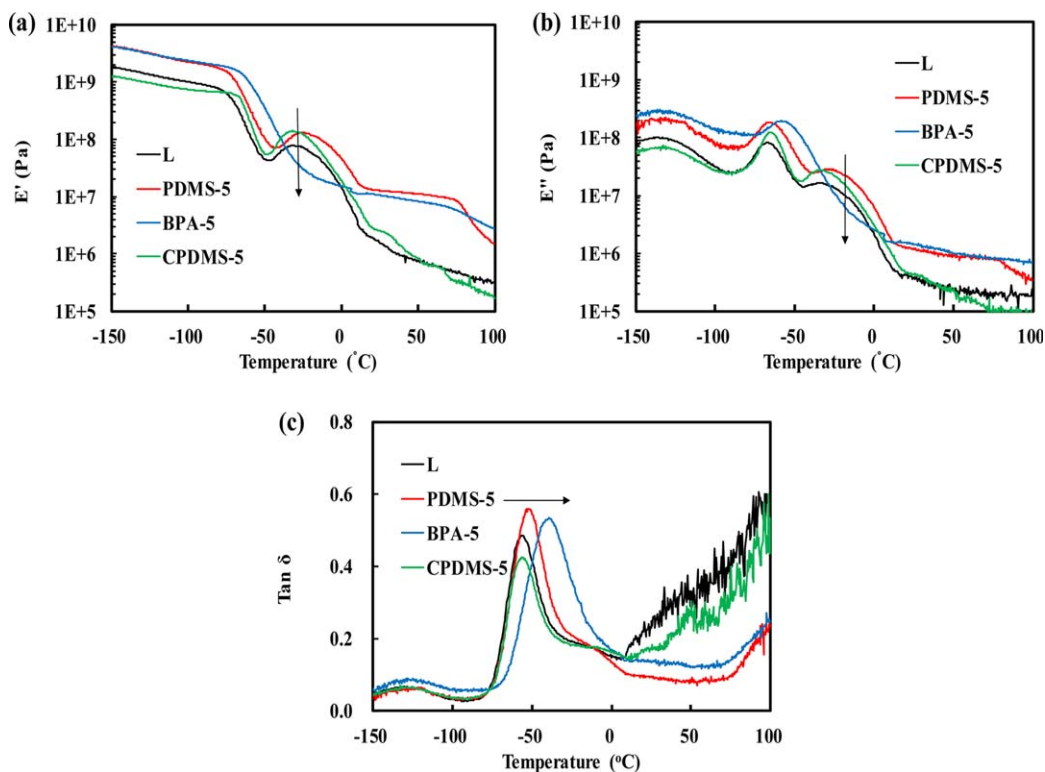


**Figure 4.** Comparison of the storage modulus ( $E'$ ) (a), loss modulus ( $E''$ ) (b), and  $\tan \delta$  (c) profiles of the PDMS-5, BPA-5, and CPDMS-5 series. [Color figure can be viewed in the online issue, which is available at [wileyonlinelibrary.com](http://wileyonlinelibrary.com).]

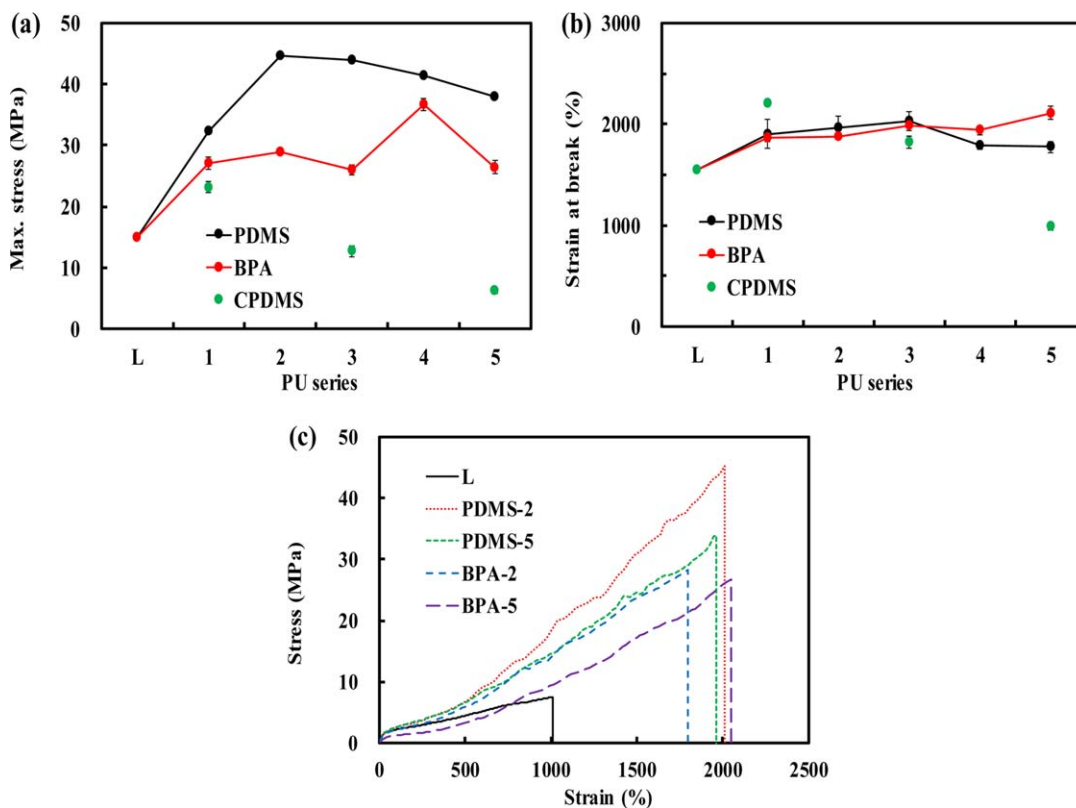


**Figure 5.** Profiles of (a) maximum stress and (b) strain at break for the PDMS, BPA, and CPDMS series, and (c) stress-strain curves of the PDMS and BPA series compared with that of L. [Color figure can be viewed in the online issue, which is available at [wileyonlinelibrary.com](http://wileyonlinelibrary.com).]

**Table III.** Shape Memory Properties of PDMS- or BPA-Linked PU Series

Sample code	Recovery (%)	Retention (%)
L	89	94
PDMS-1	88	91
PDMS-2	90	97
PDMS-3	90	90
PDMS-4	90	94
PDMS-5	91	97
BPA-1	85	93
BPA-2	91	95
BPA-3	92	93
BPA-4	96	87
BPA-5	96	72
CPDMS-1	89	97
CPDMS-3	91	85
CPDMS-5	91	88

The cold crystallization peak results also demonstrated that the interactions between soft segments were significantly affected by the linked BPA. The  $\tan \delta$  profile in Figure 4(c) shows an obvious peak shift only for BPA-5. The DSC and DMA analysis results suggested that the soft segment melting and the soft segment interactions of PU were more significantly affected by the linked BPA in the BPA series than by the linked PDMS in the PDMS series.

### Tensile and Shape Memory Properties

The maximum tensile stress of the PDMS series significantly increased compared with that of plain PU (L). However, the values of the maximum tensile stress of the BPA series were not comparable to those of the PDMS series [Figure 5(a)]. For example, 7.0 MPa for L sharply increased to 44.7 MPa for PDMS-3 and 37.9 MPa for PDMS-5 and moderately increased to 26.4 MPa for BPA-5. The maximum tensile stress increase of the PDMS series was due to the light chemical cross-linking by

the flexible PDMS, as shown in Scheme 1(b), whereas the BPA series did not form a similar degree of cross-linking because of the rigid structure of BPA, as demonstrated in the cross-link density results (Figure 1). However, the CPDMS series exhibited very low maximum tensile stress, which suggested that the addition of NaH for the deprotonation of the carbamate bonding did not aid the cross-linking of PU chains by epoxy end groups. The strain at break of the PDMS and BPA series also increased as the PDMS or BPA content increased: a value of 930% for L was increased to 1775% for PDMS-5 and 2108% for BPA-5 [Figure 5(b)]. A significant strain difference between the PDMS and BPA series was not observed, although the light cross-linking in the PDMS series was expected to restrict the stretching of the PU chains more than in the BPA series. The linked PDMS in the PDMS series and the linked BPA in the BPA series did not hinder the stretching of PU chains because the soft segment involved in the stretching was not affected by the linking of PDMS or BPA. The improved tensile properties of the PDMS and BPA series compared with those of the L form can be found in the stress-strain curves in Figure 5(c). The tensile properties of the PDMS series were comparable to those of PUs with flexible cross-linking. The PEG cross-linked PU exhibited a maximum stress of 56 MPa and a strain at break of 1568%,<sup>28</sup> and the PDMS cross-linked PU showed a maximum stress of 53 MPa and a strain at break of 1407%.<sup>29</sup> The tensile test results revealed that the light cross-linking in the PDMS series significantly improved the tensile properties compared with the BPA linking in the BPA series.

Shape recovery tests were conducted for the PDMS and BPA series at 45 °C and are summarized in Table III. The shape recoveries of the PDMS and BPA series remained above 90% as the PDMS or BPA content increased, and the CPDMS series also exhibited shape recovery above 90%. The shape retention of the PDMS series at -25 °C did not decrease below 90%, and that of the CPDMS series slightly decreased as the PDMS content increased. However, the shape retention of the BPA series significantly decreased at -25 °C as the BPA content increased, as shown by the shape retention of BPA-1 (93%) decreasing to

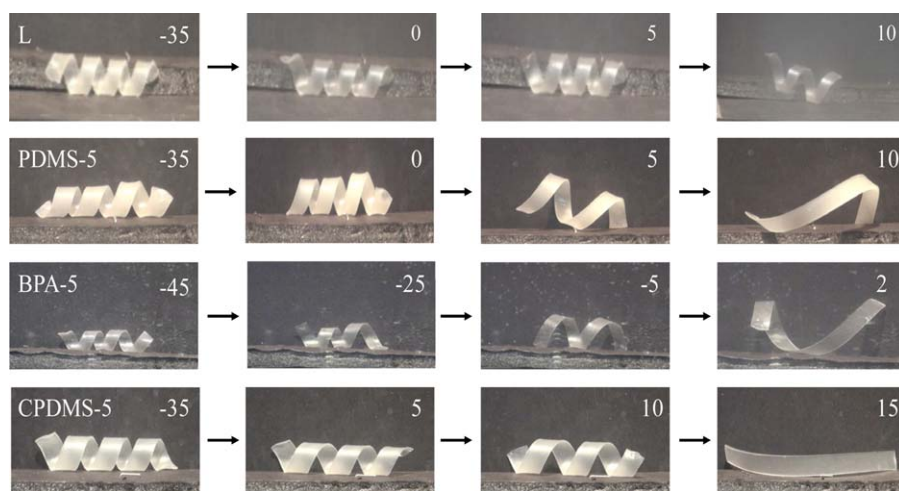


**Figure 6.** Comparison of the low-temperature flexibilities of L, PDMS-5, BPA-5, and CPDMS-5 (the numbers represent the test temperatures). [Color figure can be viewed in the online issue, which is available at [wileyonlinelibrary.com](http://wileyonlinelibrary.com).]



72% for BPA-5. The significant decrease in the shape retention of the BPA series is related to the disruption of PU chain packing by the linked rigid BPA, as observed in the DSC and DMA results. The reduction of shape retention in PU was observed when a rigid group such as cholesterol was linked to PU, which was in line with the BPA series.<sup>16</sup> Based on the tensile test and shape memory results, the linking of PDMS to PU remarkably increased the tensile strength, and the linking of BPA to PU significantly reduced the shape retention properties.

#### Low-Temperature Flexibility

The low-temperature flexibilities of selected PDMS and BPA series samples (PDMS-5, BPA-5, and CPDMS-5) were compared with that of L in Figure 6. Twisted-spiral samples were bound and stored for 3 h in a temperature-controlled chamber at  $-35^{\circ}\text{C}$  for L, PDMS-5, and CPDMS-5 and at  $-45^{\circ}\text{C}$  for BPA-5. The samples were allowed to regain their original shapes as the surrounding temperature was increased. The low-temperature flexibilities clearly differed between each sample: BPA-5 started unwinding at  $-25^{\circ}\text{C}$ , whereas L, PDMS-5, and CPDMS-5 required warming above  $5^{\circ}\text{C}$  to start unwinding. BPA-5 exhibited considerable unwinding even at  $-5^{\circ}\text{C}$ , and near-full recovery was observed at approximately  $2^{\circ}\text{C}$ , although it was frozen at  $-45^{\circ}\text{C}$ . However, the low-temperature recovery of PDMS-5 and CPDMS-5 that contained the PDMS was not superior to that of the L form. Therefore, it was demonstrated that the linked BPA rather than PDMS was effective at improving the low-temperature flexibility of PU by hindering the molecular interactions between PUs because of the bulky and rigid structure of BPA attached to PU. Therefore, the low-temperature flexibility can be improved by reducing the molecular interactions between PUs and allowing motional freedom at low temperatures, whereas ordinary polymers lose their flexibility below  $T_g$  because their rotational and vibrational movements are restricted. Previously, specialty polymers with low-temperature flexibility adopted methods such as plasticizer blending,<sup>30</sup> the addition of aliphatic oil,<sup>18</sup> and the incorporation of alkoxyated fatty acid;<sup>31</sup> however, the linking of rigid functional groups onto PU is different from the previous approaches. These findings can be used in the development of polymers that maintain their flexibility under freezing conditions.

#### CONCLUSIONS

PDMS (PDMS series) or BPA (BPA series) was linked to PU using their epoxy end groups, and the two series were compared with respect to their spectroscopic, thermal, tensile, shape memory, and low-temperature flexibility properties. The cross-link density of the PDMS series slightly increased as the PDMS content increased; however, the BPA series exhibited a sharp decrease as the BPA content increased. The soft segment  $T_m$  of the PDMS series did not vary with the PDMS content, whereas the BPA series lost its soft melting peak as the BPA content increased. The  $T_g$  of the BPA series increased as the BPA content increased, whereas the  $T_g$  of the PDMS series remained the same. The soft segment crystallization peaks for the BPA series at approximately  $-20^{\circ}\text{C}$  in the DMA results disappeared as the BPA content increased. However, the crystallization peaks for

the PDMS and CPDMS series did not decrease with increasing PDMS content. The tensile strength of the PDMS series significantly increased as the PDMS content increased, whereas that of the BPA series exhibited a moderate increase. The shape recovery of the BPA series at  $45^{\circ}\text{C}$  remained over 90%; however, the shape retention at  $-25^{\circ}\text{C}$  decreased as the BPA content increased. The BPA series demonstrated excellent low-temperature flexibilities compared with the PDMS and CPDMS series. Therefore, the differences between the PDMS and BPA series in thermal, tensile, shape memory, and low-temperature flexibility properties originated from the rigid aromatic structure of BPA compared with the flexible PDMS structure.

#### ACKNOWLEDGMENTS

This study was supported by the R&D Center for Valuable Recycling (Global-Top Environmental Technology Development Program) funded by the Ministry of Environment (Project No.: GT-11-C-01-040-0). This work was supported by the 2015 Inje University research grant.

#### REFERENCES

1. Staples, C. A.; Woodburn, K.; Caspers, N.; Hall, A. T.; Klečka, G. M. *Hum. Ecol. Risk Assess.* **2002**, *8*, 1083.
2. Maeda, Y.; Paul, D. R. *J. Polym. Sci. Polym. Phys.* **1987**, *25*, 1005.
3. Maw, D. J.; Huang, C. C.; Maw, B. Y. *Polymer* **1998**, *39*, 3529.
4. Tsi, H. Y.; Chen, C. C.; Tsen, W. C.; Shu, Y. C.; Chuang, F. S. *Polym. Test.* **2011**, *30*, 50.
5. Park, J. H.; Park, K. D.; Bae, Y. H. *Biomaterials* **1999**, *20*, 943.
6. Soldani, G.; Losi, P.; Bernabei, M.; Burchielli, S.; Chiappino, D.; Kull, S.; Briganti, E.; Spiller, D. *Biomaterials* **2010**, *31*, 2592.
7. Pergal, M. V.; Dzunuzovic, J. V.; Poreba, R.; Ostojic, S.; Radulovic, A.; Špirková, M. *Prog. Org. Coat.* **2013**, *76*, 743.
8. Jingjing, H.; Weilin, X. *Appl. Surf. Sci.* **2010**, *256*, 3921.
9. Chunli, H.; Miao, W.; Xianmei, C.; Xiaobo, H.; Li, L.; Haomiao, Z.; Jian, S.; Jiang, Y. *Appl. Surf. Sci.* **2011**, *258*, 755.
10. Alves, P.; Coelho, J. F. J.; Haack, J.; Rota, A.; Bruinink, A.; Gil, M. H. *Eur. Polym. J.* **2009**, *45*, 1412.
11. Chung, Y. C.; Jung, I. H.; Choi, J. W.; Chun, B. C. *Polym. Bull.* **2014**, *71*, 1153.
12. Tan, K.; Obendorf, S. K. *J. Mem. Sci.* **2007**, *289*, 199.
13. Seymour, R. B.; Kauffman, G. B. *J. Chem. Ed.* **1992**, *69*, 909.
14. Meier-Westhues, U. In *Polyurethanes-Coatings, Adhesives, and Sealants*; Vincentz Network: Hannover, **2008**.
15. Oertel, G. In *Polyurethane Handbook*; Hanser: Munich, **1994**.
16. Chung, Y. C.; Kim, H. Y.; Yu, J. H.; Chun, B. C. *Macromol. Res.* **2015**, *23*, 350.

17. Zook, J. D.; DeMoss, S.; Jordan, D. W.; Rao, C. B. U.S. Patent 6,172,179 B1 (2001).
18. Theodore, A. N.; Killgoar, Jr.; P. C. U.S. Patent 4,853,428 A (1987).
19. Kim, B. K.; Shin, Y. J.; Cho, S. M.; Jeong, H. M. *J. Polym. Sci. Polym. Phys.* **2000**, *38*, 2652.
20. Lee, B. S.; Chun, B. C.; Chung, Y. C.; Sul, K. I.; Cho, J. W. *Macromolecules* **2001**, *34*, 6431.
21. Liu, Y.; Ni, Y.; Zheng, S. *Macromol. Chem. Phys.* **2006**, *207*, 1842.
22. Petrovic, Z. S.; Javni, I.; Divjakovic, V. *J. Polym. Sci. Polym. Phys.* **1998**, *36*, 221.
23. Sekkar, V.; Gopalakrishnan, S.; Ambika Devi, K. *Eur. Polym. J.* **2003**, *39*, 1281.
24. Sekkar, V.; Rama Rao, M.; Krishnamurthy, V. N.; Jane, S. R. *J. Appl. Polym. Sci.* **1996**, *62*, 2317.
25. Choi, T.; Weksler, J.; Padsalgikar, A.; Runt, J. *Polymer* **2010**, *51*, 4375.
26. Russo, P.; Lavorgna, M.; Piscitelli, F.; Acierno, D.; Di Maio, L. *Eur. Polym. J.* **2013**, *49*, 379.
27. Hashimoto, T.; Umehara, A.; Urushisaki, M.; Kodaira, T. *J. Polym. Sci. Polym. Chem.* **2004**, *42*, 2766.
28. Chung, Y. C.; Nguyen, D. K.; Chun, B. C. *Polym. Eng. Sci.* **2010**, *50*, 2457.
29. Chung, Y. C.; Park, H. S.; Choi, J. W.; Chun, B. C. *High Perform. Polym.* **2012**, *24*, 200.
30. Ellul, M. D. U.S. Patent 5,290,886 A (1994).
31. Nissen, D.; Schmidt, H. U.; Straehle, W.; Schuett, U.; Marx, M. U.S. Patent 4,383,050 A (1983).